

## **General Disclaimer**

### **One or more of the Following Statements may affect this Document**

- This document has been reproduced from the best copy furnished by the organizational source. It is being released in the interest of making available as much information as possible.
- This document may contain data, which exceeds the sheet parameters. It was furnished in this condition by the organizational source and is the best copy available.
- This document may contain tone-on-tone or color graphs, charts and/or pictures, which have been reproduced in black and white.
- This document is paginated as submitted by the original source.
- Portions of this document are not fully legible due to the historical nature of some of the material. However, it is the best reproduction available from the original submission.

X-646-71-344  
PREPRINT

NASA TM X-~~65678~~

# TILT-ANGLE DEPENDENCE OF 10 MEV PROTON CUTOFF LATITUDES

JAMES L. BURCH

AUGUST 1971



GODDARD SPACE FLIGHT CENTER  
GREENBELT, MARYLAND

FACILITY FORM 602

(ACCESSION NUMBER)	N71-33444	(THRU)	63
(PAGES)	19	(CODE)	24
(NASA CR OR TMX OR AD NUMBER)	TMX- <del>65678</del>	(CATEGORY)	

TILT-ANGLE DEPENDENCE  
OF 10 MEV PROTON  
CUTOFF LATITUDES

By

James L. Burch  
Science Research Laboratory  
and Department of Physics  
U.S. Military Academy  
West Point, New York 10996

AUGUST 1971

---

\*Present Address: Code 646, NASA-Goddard Space Flight Center, Greenbelt,  
Maryland 20771

## TILT-ANGLE DEPENDENCE OF 10 MEV PROTON CUTOFF LATITUDES

James L. Burch

### ABSTRACT

Trajectories of 10 Mev protons in an image dipole model magnetosphere have been numerically integrated for several values of the tilt of the geomagnetic dipole. In order to obtain a closed magnetic field model it is necessary to tilt the image dipole toward the earth for northern hemisphere summer conditions. Significant variations in cutoff latitude with changing tilt angle are found only near 0600 and 1600 local times with cutoff latitudes closest to the pole for the zero tilt condition.

## INTRODUCTION

It has been known for some time that energetic particle cutoff latitudes are in fact much lower than predicted by Stoermer's dipole field calculations. Numerical integration of charged particle trajectories in the Taylor-Hones and Williams-Mead geomagnetic models by Taylor (1967), Gall et al (1968) and Smart et al (1969) have shown that much better approximations to true cutoff values can be made by using these more realistic magnetic field models. If accurate cutoffs for a given geographic location are to be obtained for the more energetic particles, a spherical harmonic expansion is needed to represent the earth's internal magnetic sources (see, e.g., Shea et al, 1965). For the lower energy particles (for example, solar protons with energies less than about 20 Mev) an accurate representation of the outer magnetosphere and polar regions are more important considerations.

The Taylor-Hones and Williams-Mead models have been handicapped by the difficulty in representing accurately the magnetic effects produced near the earthward boundary of the neutral sheet current and by the inability to allow for the changing tilt of the geomagnetic axis with respect to the ecliptic plane. Olson (1969) has recently adapted the self-consistent field model of Mead and Beard (1964) to oblique solar wind incidence, thereby providing a representation of the magnetopause for all solar wind incidence angles. By appropriate integration of the predicted boundary currents it is possible to calculate the magnetic field anywhere inside. It is generally conceded that the Olson and Williams-Mead models, which are based on a solar-wind pressure-balance formulation, are the most physically meaningful and offer greater potential as the basis of a

possible "real-time" magnetospheric model. However, once an appropriate image dipole has been found, the mathematical simplicity of the Taylor-Hones model makes it a valuable tool for calculations such as the integration of particle trajectories violating one or more adiabatic invariants. For such particles the determination of a single trajectory requires values for the magnetic induction vector at tens of thousands of locations within the magnetosphere.

The purpose of this study is to adapt the Taylor-Hones model to arbitrary tilt angles and to investigate the resulting seasonal and diurnal effects on calculated energetic particle trajectories. The basic Taylor-Hones parameters are retained; that is, an image dipole 28 times as strong as the earth's dipole is placed at a geocentric distance of  $40 R_E$ . Magnetospheric electric fields have not been incorporated into this model, but their effects will be negligible for the 10 Mev protons investigated.

#### MAGNETIC FIELD MODEL

It is well-known (see, e.g., Maxwell, 1881; Chapman and Ferraro, 1931) that the effects of an infinite conducting plane moving toward a magnetic dipole can be reproduced by replacing the conductor with an image dipole of equal moment placed an equal distance behind the plane. The effect is to confine all the magnetic flux from each dipole to the half-space bounded by the conducting plane. The method works equally well for dipoles which are tilted with respect to the conducting plane as long as a true mirror image orientation is maintained by tilting the image dipole an equal amount in the opposite direction. Although it is known that the solar wind does not act like a moving, infinite conducting plane, it was found

by Hones (1963) that the addition to the earth's field of a much stronger image dipole placed a greater distance away gives a fairly accurate representation of the dayside magnetosphere. Actually the method would be more suitably named the immersed dipole model in which the weaker (earth's) dipole is confined to a bulged-out cavity in the stronger field.

As long as the two dipole fields share a common equatorial plane flux is conserved within each field. However, if the smaller dipole is tilted, interconnection of the two dipole fields occurs. This effect has been illustrated by Antonova and Shabansky (1968). It is not thought possible to eliminate the interconnection completely, but it can be minimized by finding an optimum relative orientation for the two dipoles. As mentioned above, for dipoles of equal magnitudes, the mirror image orientation is correct. Such a method was tried as a first approximation to the northern hemisphere summer configuration but resulted in a large loss of flux from a region several degrees wide near the southern neutral point. Other possible methods were suggested by the following features of the equal dipole orientation: (1) The magnetic torques experienced by the two dipoles are equal in magnitude and are in opposite directions, (2) The radial component of the total field vanishes at the subsolar point, (3) The neutral points lie on the same undisturbed dipole field line. The zero total torque approach was dismissed since it requires equal tilt angles and this method was found not to conserve flux as described above. A similar approach was used by Sauer (private communication) who chose an orientation which produced zero torque on the earth's dipole. This method also was not pursued since it does not conserve flux in the equal dipole case (see (1)

above). Requiring a total field perpendicular to the ecliptic plane at the subsolar point (assumed at  $10.8 R_E$  geocentric distance) gives image dipole tilt angles of  $7.0^\circ$ ,  $10.5^\circ$  and  $14.0^\circ$  for earth dipole tilts of  $10^\circ$ ,  $15^\circ$  and  $20^\circ$  respectively and these values were used as first approximations. Recognizing that complete flux conservation is not possible, a field line tracing program was used to test neighboring orientations to minimize the region of flux loss at the noon meridian. Field line tracing was also performed for other local times until confidence was gained that within practical limits flux loss was very nearly minimized. This procedure resulted in regions of flux loss in the noon-meridian plane less than  $0.6^\circ$  wide in invariant latitude. Image dipole tilt angles obtained by this method are  $6.84^\circ$ ,  $10.28^\circ$  and  $13.83^\circ$  for  $10^\circ$ ,  $15^\circ$  and  $20^\circ$  earth dipole tilts. These optimum values were found to the nearest  $.01^\circ$  using a program which follows each line of force in segments  $.01 R_E$  in length. The resulting neutral points were found to lie on undisturbed dipole field lines whose invariant latitudes differed by less than  $0.5^\circ$  (see (3) above), giving further assurance that a near-optimum configuration had been attained.

A neutral sheet field was added to the two dipole fields as follows: A semi-infinite neutral plane was taken parallel to the ecliptic plane with termination at a distance of  $8 R_E$  in the geomagnetic equatorial plane. Edge effects were neglected and a zero field addition was assumed in the region within  $0.25 R_E$  above and below the neutral sheet, allowing field line connection as produced by the two dipole fields. At larger distances above and below the neutral sheet a solar-antisolar field was added. This

field had a magnitude of  $30y$  at the earthward edge of the neutral sheet and decreased with distance down the tail in proportion to  $x_{SE}^{-0.3}$ , where  $x_{SE}$  is the distance downstream of the earth (see Behannon, 1968). As shown by Antonova and Shabansky (1968) the inclusion of edge effects of the neutral sheet current in the zero-tilt model will move the neutral points to lower invariant latitudes in better agreement with experiment. These effects were not included in the present model, it being decided that, due to uncertainties in the near-earth configuration of the neutral sheet for tilted conditions, the large asymmetry of the additional field contributions would only complicate the selection of an optimum dipole configuration while adding questionable validity to the model.

Several noon-midnight field lines are shown in Figure 1 for a tilt of  $15^\circ$  and northern hemisphere summer conditions. Using solar-wind pressure-balance calculations, Spreiter and Sriggs (1962) and Olson (1969) have found that the shape of the magnetopause depends very little upon the tilt angle except near the neutral points. Although the zero-tilt neutral points of the Taylor-Hones model lie several degrees closer to the solar ecliptic plane than those of Olson's model, their relative displacements as the tilt angle is changed are roughly the same. For example, during northern summer conditions with a  $10^\circ$  tilt, the present model predicts that the angle between the radius vector to the northern neutral point and the earth-sun line will be reduced by  $9.3^\circ$  while the corresponding angle in the southern hemisphere will be increased by  $8.8^\circ$ . The northern and southern values reported by Olson (1969) are  $8.0^\circ$  and  $8.9^\circ$  respectively. For a  $15^\circ$  tilt the northern and southern neutral points are shifted by

$13.0^\circ$  and  $12.5^\circ$  respectively, compared to displacements of  $11.2^\circ$  and  $14.0^\circ$  in Olson's model.

PARTICLE TRAJECTORY COMPUTATIONS

10 Mev protons were chosen for a study of the effects of the tilted field on energetic particle cutoff latitudes. In addition to their importance in solar flare effects, they are of high enough energy that the neutral sheet and electric field inadequacies of the model magnetosphere are obviated while still having high enough cutoff latitudes that some tilt effects should be evident. The trajectory tracing routine is similar to that described by Taylor (1967). The fourth-order Runge-Kutta program published in the IBM System/360 Scientific Subroutine Package (360A-CM-03X) Version II was used to trace backward the trajectory of a proton arriving along the field line at 1000 km altitude. Calculations were carried out on the U.S. Military Academy's General Electric 635 computer using double-precision arithmetic throughout to reduce roundoff errors. A maximum step size of one-tenth the local Larmor radius ( $R_L$ ) was used and an accuracy check was made in every step requiring that halving of the step size produced a position difference less than  $(2 \times 10^{-5})R_{L1000\text{ km}}$ . This assured a maximum error for 50,000 numerical steps on the order of the 1000 km Larmor radius. The program was successfully tested for particle motion in a uniform field and calculations for the zero-tilt field were found to be in agreement with independent results provided by Dr. H. E. Taylor.

With the above assurances of the program's reliability it was used to integrate equations of motion of 10 Mev "negative" protons directed upward along the local magnetic induction vector at 1000 km altitude.

In all, 440 trajectories were traced in determining cutoff latitudes for tilts of  $0^\circ$ ,  $\pm 10^\circ$  and  $\pm 20^\circ$  at various local times. At a given local time an initial latitude was selected at which a particle directed up the field line would intersect the atmosphere (altitude < 100 km) before reaching its first mirror point. The latitude was then increased in intervals of  $0.1^\circ$  until the proton either crossed the magnetopause or reached a path length of  $50 R_E$  without returning to 100 km altitude. Intersection with the atmosphere indicated that the starting latitude was inaccessible to zero-pitch-angle protons from infinity. Crossing of the magnetopause was taken to indicate an allowed trajectory. However, most trajectories analyzed had successive mirror points progressively higher above the atmosphere and reached a path length of  $50 R_E$  inside the magnetosphere. These latitudes were considered to be allowed to the extent that they are accessible to protons with certain mirror points in the outer magnetosphere. They are strictly accessible then only if some type of field line merging or diffusion process allows the protons free access through the tail to the outer magnetosphere since it has been found by Gall et al (1968) that 10 Mev protons cannot cross the compressed dayside boundary. Occasionally a penumbral type behavior was noted near the cutoff latitude. In all cases the cutoff latitude was taken as the lowest latitude at which an allowed orbit was found.

Table 1 lists cutoff latitudes for 0600 and 1500 local times. All calculations were made for northern hemisphere summer conditions with the negative tilt values indicating southern hemisphere calculations (winter conditions). As indicated by these values, when a significant tilt

dependence is found (greater than a few tenths of a degree), it is always such that the  $0^\circ$  cutoff lies closest to the pole. In Figure 2 are plotted the cutoff latitudes for  $0^\circ$  tilt and  $+20^\circ$  tilt. The local-time dependence for  $0^\circ$  tilt is similar, although, as expected, not as pronounced as that found by Taylor (1967) for zero-pitch-angle 1.2 Mev protons. Cutoff latitudes for  $+20^\circ$  tilt are shown to be displaced to lower latitudes at local times near 0600 and 1600 while at other local times no significant difference is noted.

#### DISCUSSION

There have been no published reports of attempts to measure the tilt dependence of low-energy cosmic ray cutoff latitudes. Such a study for solar cosmic rays would be difficult to perform since appreciable fluxes are typically found during disturbed periods when the earth's magnetic field is highly distorted and variable. However, some unexplained seasonal and longitudinal variations have been found in the position of the galactic cosmic ray knee which occurs at the approximate cutoff latitude of 600 Mev protons. George (1970) has noted some tendency for the cosmic ray knee to lie slightly closer to the pole during winter time. Such behavior is not predicted by this study. Seward and Kornblum (1965) have found a large longitudinal dependence in the position of the northern hemisphere knee at local times within three hours of noon and midnight for relatively quiet geomagnetic conditions ( $K_p \leq 3+$ ). The northern hemisphere knee was farthest from the pole near  $120^\circ E$  longitude and closest to the pole near  $30^\circ E$  longitude. All observations were made near equinox conditions,

September 18 to 22, 1961. Assuming the north magnetic pole to be at  $69^{\circ}\text{W}$  and  $78.5^{\circ}\text{N}$  (see, e.g., Chapman and Bartels, 1940) we find that when it is midnight at  $120^{\circ}\text{E}$  it is very nearly noon at  $69^{\circ}\text{W}$ , producing a condition of maximum daily tilt toward the sun. The maximum tilt away from the sun likewise occurs when it is noon at  $120^{\circ}\text{E}$ . Similarly noon and midnight at  $30^{\circ}\text{E}$  correspond approximately to dawn and dusk at  $69^{\circ}\text{W}$ , or the two minimum tilt configurations. In Figure 3 Seward and Kornblum's longitude plot has been converted to a tilt angle one. For the purposes of this plot it is assumed that all observations were made exactly at noon or midnight. Tilt angles shown are the complements of the angles between the centered dipole and the earth-sun line for equinox conditions. There is seen a definite tendency for the knee to lie nearer the pole at  $0^{\circ}$  tilt. Seward and Kornblum's southern hemisphere data were handicapped by a large gap due to the Atlantic Anomaly, preventing a determination of the longitudinal dependence for southern latitudes.

Although no significant tilt variations were found in the present study for protons arriving along the magnetic field vector at noon and midnight, the arrival of protons at larger pitch angles may show a larger tilt dependence. It is also possible that the Seward and Kornblum observations can be explained by internal magnetic effects. However, calculations using sixth-degree internal field simulations (see, e.g., Shea et al, 1965, and Smart et al, 1969) have not predicted such a behavior.

A comprehensive study of these effects should include accurate neutral sheet and ring current models for tilted conditions and calculations for different pitch angles. An accurate study for higher energy particles should also include a high-order simulation of the internal field enabling one to separate longitudinal effects from those due to the changing tilt angle.

#### ACKNOWLEDGMENTS

I am grateful to Lt. Col. William B. Streett, Director of the Science Research Laboratory, for much support and encouragement. This work could not have been completed without the large amount of computer time generously provided by the U.S.M.A. Academic Computer Center. I also wish to thank Dr. H. E. Taylor for providing sample trajectory calculations.

### REFERENCES

Antonova, A. E., and V. P. Shabansky, On the structure of the geomagnetic field at large distances from the earth, Geomagnetism and Aeronomy, 8, 801-811, 1968.

Behannon, K. W., Mapping of earth's bow shock and magnetic tail by Explorer 33, J. Geophys. Res., 73, 907-930, 1968.

Chapman, S., and Julius Bartels, Geomagnetism, Vol. II, 648, Oxford, 1940.

Chapman, S., and V. C. A. Ferraro, A new theory of magnetic storms, Terrest. Magnetism and Atmospheric Elec., 36, 77-97 and 171-186, 1931.

Gall, Ruth, Jaime Jimenez, and Lucilla Camacho, Arrival of low-energy cosmic rays via the magnetospheric tail, J. Geophys. Res., 73, 1593-1605, 1968.

George, Michael J., Observations of the cosmic ray knee with a polar orbiting ionization chamber, J. Geophys. Res., 75, 3159-3166, 1970.

Hones, Edward W., Jr., Motions of charged particles trapped in the earth's magnetosphere, J. Geophys. Res., 68, 1209-1219, 1963.

Maxwell, J. C., Electricity and Magnetism, 2d. ed., Ch. XII, Par. 657, Oxford, 1881.

Mead, G. D., and D. B. Beard, Shape of the geomagnetic field - solar wind boundary, J. Geophys. Res., 69, 1169-1179, 1964.

Olson, W. P., The shape of the tilted magnetopause, J. Geophys. Res., 74, 5642-5651, 1969.

Seward, F. D., and H. N. Kornblum, Jr., Near-earth, polar-orbiting satellite measurements of charged particles, 1. Instrumentation and cosmic rays. J. Geophys. Res., 70, 3557-3570, 1965.

- 2 -

Shea, M. A., D. F. Smart, and K. G. McCracken, A study of vertical cutoff rigidities using sixth degree simulations of the geomagnetic field, J. Geophys. Res., 70, 4117-4130, 1965.

Smart, D. F., M. A. Shea, and Ruth Gall, The daily variation of trajectory-derived high-latitude cutoff rigidities in a model magnetosphere, J. Geophys. Res., 74, 4731-4738, 1969.

Spreiter, John R., and Benjamin R. Briggs, Theoretical determination of the form of the boundary of the solar corpuscular stream produced by interaction with the magnetic dipole field of the earth, J. Geophys. Res., 67, 37-51, 1962.

Taylor, Harold E., Latitude local-time dependence of low-energy cosmic-ray cutoffs in a realistic geomagnetic field, J. Geophys. Res., 72, 4467-4470, 1967.

### FIGURE CAPTIONS

Table 1: Geomagnetic cutoff latitudes for 10 Mev protons at several tilt angles. All calculations were made for northern hemisphere summer conditions. Negative tilt angles indicate southern hemisphere values (winter conditions).

Figure 1: Several magnetic field lines for a tilt angle of  $+15^\circ$  (northern hemisphere summer conditions). The earth's dipole axis lies along the vertical. Indicated latitudes are geomagnetic latitudes at which field lines intersect the earth's surface.

Figure 2: Local time and tilt angle dependence of cutoff latitudes for 10 Mev protons arriving at 1000 km along the field line. Open circles indicate zero tilt angle. Solid circles indicate  $+20^\circ$  tilt angle (summer conditions). Half-solid circles indicate a difference of less than a few tenths of a degree (the typical penumbral band width). Shaded regions show approximate latitudes which are forbidden for  $0^\circ$  tilt but allowed for  $+20^\circ$  tilt.

Figure 3: Northern hemisphere cosmic ray knee positions taken from Seward and Kornblum (1965) and replotted in terms of tilt angle rather than longitude. Tilt angles are the complements of the angles between the centered dipole and the earth-sun line. Data points were taken within three hours of noon and midnight, but were assumed to be at exactly noon and midnight for purposes of tilt angle computations.

LOCAL TIME	TILT ANGLE	CUTOFF LATITUDE
0600	-20°	68.3°
	-10°	69.5°
	0°	70.9°
	+10°	70.1°
	+20°	68.4°
1500	-20°	68.5°
	-10°	69.2°
	0°	69.4°
	+10°	69.1°
	+20°	68.6°

TABLE 1

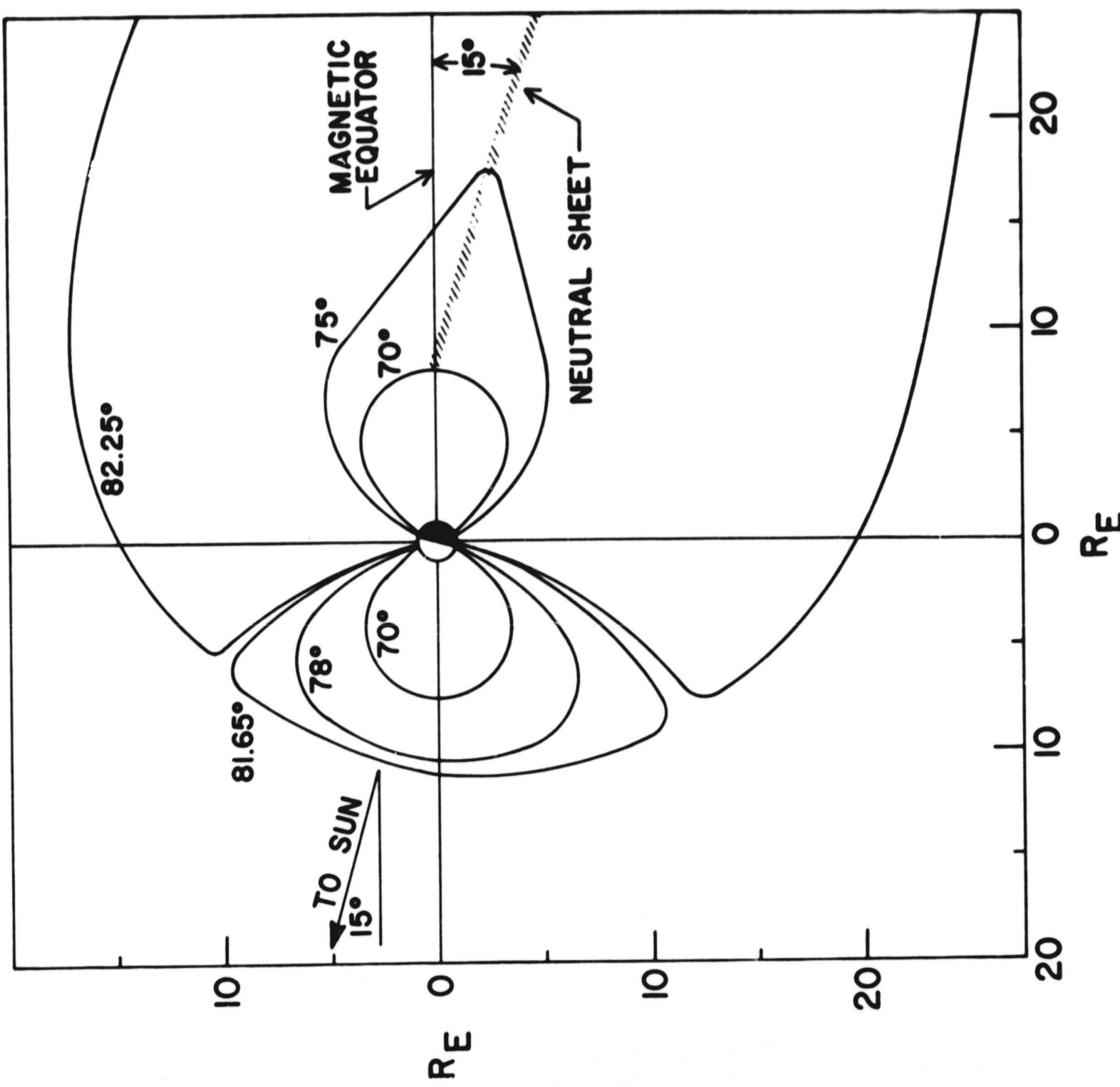


FIGURE 1

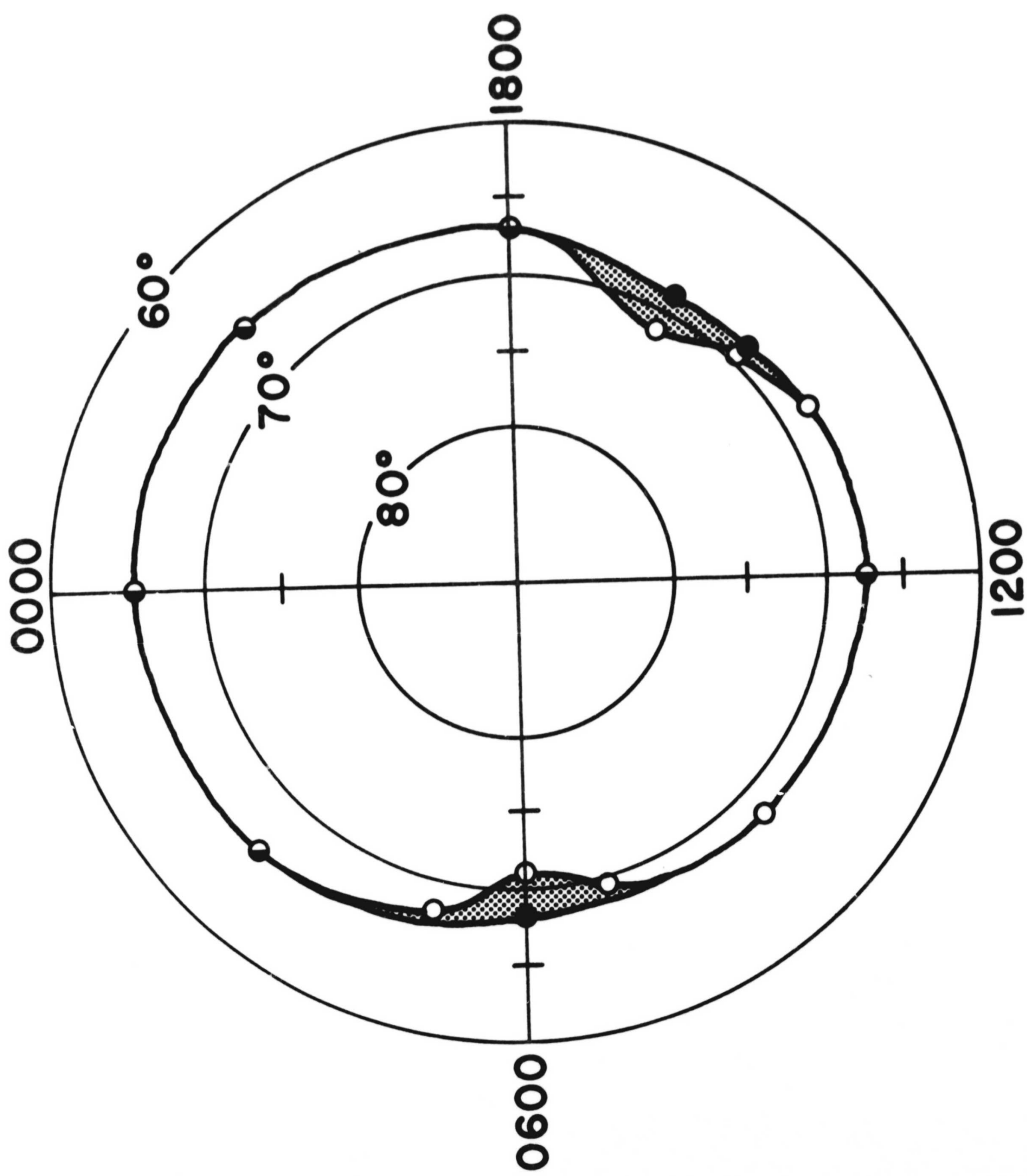


FIGURE 2

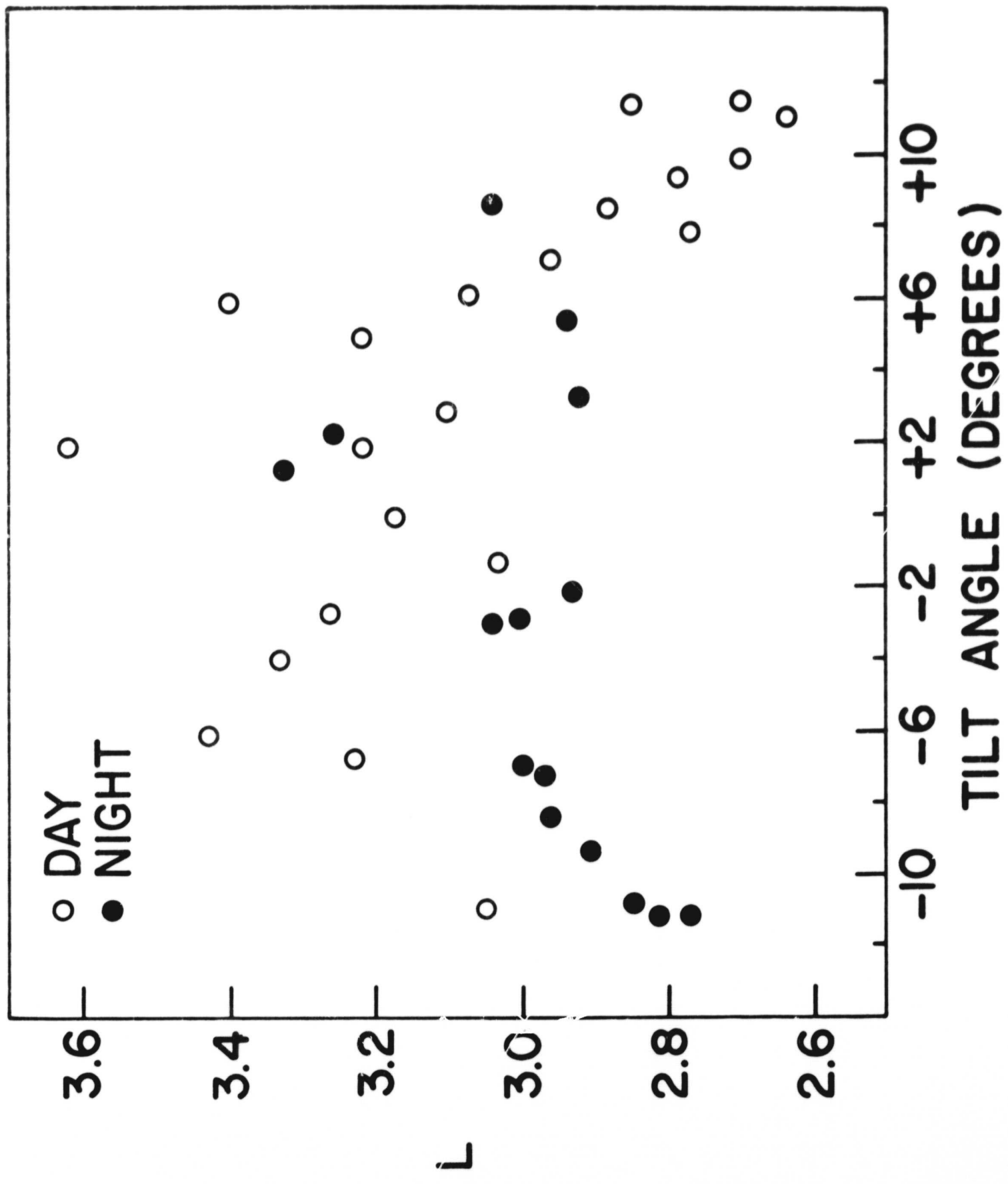


FIGURE 3